MULTINUCLEAR NMR IMAGING OF SOLIDS

J. B. Miller and A. N. Garroway

Chemistry Division, Code 6120
Naval Research Laboratory
Washington, D.C. 20375-5000

INTRODUCTION

Nuclear magnetic resonance (NMR) is a powerful analytical tool for the study of materials. The utility of NMR is derived from the unique information it provides on the physical and chemical structure of the material being studied. The ability to obtain such information as a function of spatial position within the sample makes magnetic resonance imaging (MRI) potentially an important technique for the NDE of materials [1]. In general, current MRI instrumentation and techniques limit the study of materials to cases where the observed nuclei are in a liquid-like environment. Even so, reports of imaging liquids in solid materials [2,3] and the soft components of materials [4] have appeared. To date there are few examples of MRI applied to the imaging of the solid components of materials [5].

The major limitation to the direct application of MRI methods for the study of solid materials is that the NMR linewidth is three to five orders of magnitude greater than those observed for liquids. The increased linewidth causes two problems for MRI of solids: one is a decrease in spatial resolution for given imaging parameters, and the other is a decrease in signal-to-noise ratio. A decrease in spatial resolution can in principle be overcome by changing the imaging parameters, however the ultimate limit on spatial resolution in MRI of solids is the ability to detect the NMR signal from the smallest volume element to be resolved. The signal-to-noise ratio is proportional to the observed linewidth and the number of nuclear spins within a volume element; therefore in solids the linewidth limits the spatial resolution.

The obvious solution to the linewidth problem is to narrow the lines. A number of methods for line-narrowing spin-1/2 resonances in solids are known [6] and include tailored rf excitation of the nuclei and mechanical rotation of the sample. The appropriate line-narrowing technique depends of the line-broadening mechanisms which in turn depend on the concentration of the nuclear spins within the sample. The predominant line-broadening mechanism for concentrated nuclei is homonuclear dipole-dipole coupling with generally smaller contributions from a combination of chemical shift anisotropy, isotropic chemical shift

variations, bulk susceptibility, and static magnetic field inhomogeneity, referred to here collectively as inhomogeneous effects.

For dilute spins the same inhomogeneous effects described above produce the line broadening. If a second nuclear spin is present, heteronuclear dipole-dipole couplings will contribute to or even dominate the line broadening. The heteronuclear dipolar interaction is also an inhomogeneous effect.

Several examples of line-narrowing in conjunction with MRI have appeared. Homonuclear dipolar decoupling techniques including tailored rf excitation [7] and mechanical rotation [8] have been used for obtaining ^{1}H NMR images of solids. A method for removing inhomogeneous broadening from MRI of liquids which we refer to as refocused gradient imaging (RGI) has also been demonstrated [9,10]. We describe below two variants of RGI, one suitable for imaging dilute spin-1/2 nuclei in solids, the other simultaneously removing homonuclear dipolar and inhomogeneous broadening for imaging of concentrated spins in solids.

REFOCUSED GRADIENT IMAGING

MRI is usually accomplished by recording the NMR spectrum in the presence of a static magnetic field gradient. After rf excitation the spins evolve at a rate determined by the external applied magnetic field and the various inhomogeneous interactions. In the presence of a magnetic field gradient, the phase accumulated by the spins at position z after a time τ is given by

$$\phi(z) = G_z z\tau + \omega_i \tau \qquad (1)$$

where G_z is the magnetic field gradient amplitude and ω_i is the evolution rate of the combined inhomogeneous interactions. If at time τ we apply an rf π pulse so that the signs of the spin states are interchanged [11], then the evolution rates for the field gradient and inhomogeneous interactions become $-G_z z$ and $-\omega_i$ respectively. At time 2τ, $\phi(z)$ will be zero; inhomogeneous broadening has been suppressed. Unfortunately we have also lost our spatial information. However, spatial information can be reintroduced by the use of a time-dependent field gradient such that the sign of G_z changes when the π pulse is applied. Now at time 2τ $\phi(z)$ will be $2G_z z\tau$.

Figure 1a shows schematically the RGI pulse sequence [9,10] employed for liquid state imaging. The premise of the sequence is the same as that described above, however now we use a train of π pulses [11] to generate a series of points in time, each midway between two adjacent π pulses, where the inhomogeneous interactions are zero. Transverse magnetization is sampled at these points and the resultant data are Fourier transformed to produce a 1-dimensional image of the material. Any periodic amplitude modulation of the gradient can be used with RGI; as shown in the figure, we used sinusoidal modulation to obtain the images presented here.

A demonstration of the RGI method applied to a liquid sample is shown in Fig. 1. The sample, shown as an inset to the figure, consisted of three tubes of $CoCl_2$ doped water, of approximately 1.2 mm inner diameter and separated by 0.3 mm. A steel pin could be inserted to within 9 mm of the tube labeled 1 to create the inhomogeneous broadening. Figures 1b and 1c are the standard and RGI 1-dimensional images of the sample, without inhomogeneous broadening, respectively. The three tubes

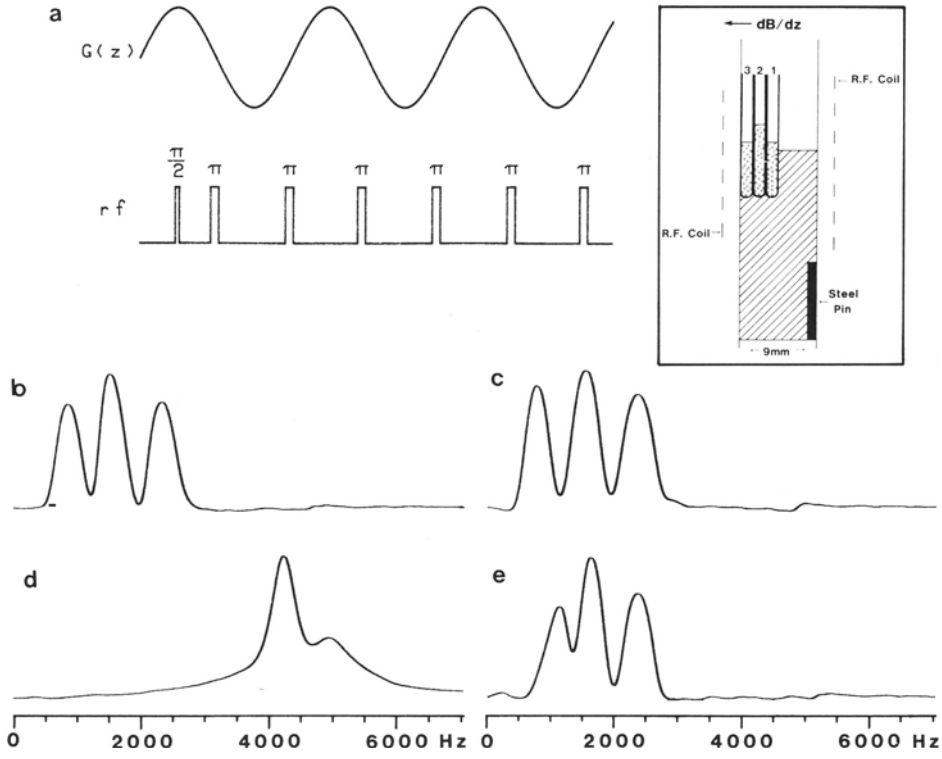

Fig. 1 Refocused gradient imaging of liquids. The sample shown in the inset consists of three tubes of $CoCl_2$ doped water 1.2 mm in diameter and separated by 0.3 mm. A steel pin could be inserted to create inhomogeneous broadening. a) RGI pulse sequence for imaging liquids; b) standard image of sample without the steel pin; c) RGI without the steel pin; d) standard image with the pin; e) RGI with the pin.

can be clearly resolved in these images. Figure 1d shows the effect of inhomogeneous broadening on the standard image of the sample. The image is distorted beyond recognition. In contrast the RGI image in Fig. 1e, obtained with the steel pin in place, provides nearly the same resolution as without the steel pin. We believe that the slight distortion of the image at tube 1 is due to distortions in the rf field caused by the close proximity of an electrically conductive object (the steel pin).

Refocused Gradient Imaging of Dilute Nuclei in Solids

In principle, the same RGI pulse sequence used to image liquids may be used to image dilute spin-1/2 nuclei in solids since in both cases only inhomogeneous broadening is present. However for many materials we will want to make the modifications shown in Fig. 2a [12]. This is the pulse sequence used to produce the natural abundance ^{13}C image of Fig. 2b. There are two main modifications to the pulse sequence. The first is that we have replaced the $\pi/2$ excitation pulse with a cross-

polarization [13] pulse to enhance the signal amplitude. The second is the inclusion of heteronuclear dipolar decoupling [14]. Although ideally the pulse sequence removes heteronuclear dipolar broadening, in practice one rarely has a sequence of ideal pulses with which to work. The effectiveness of the pulse sequence in removing inhomogeneous broadening

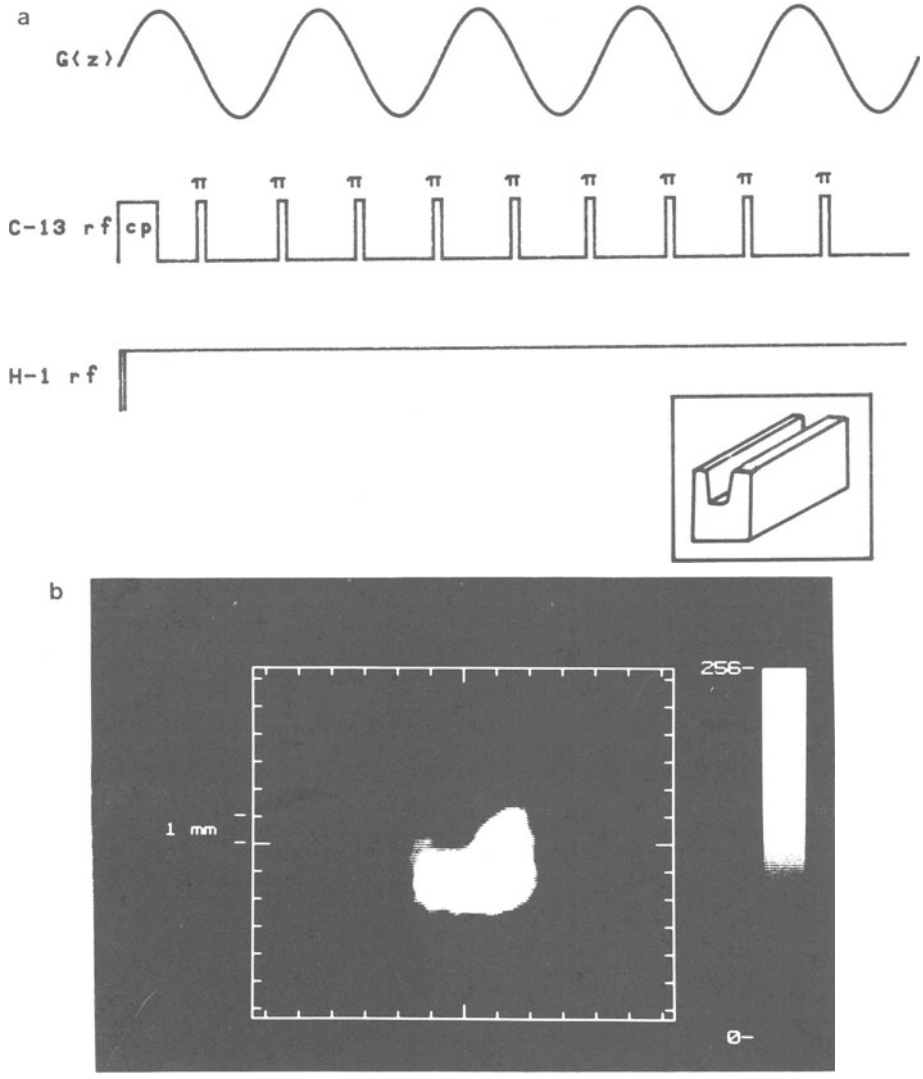

Fig. 2 Refocused gradient imaging of dilute nuclei in solids. A sample of polycarbonate with dimensions of 4.5 mm X 5.5 mm X 16 mm is shown in the inset. The plane of the page is the imaging plane. a) The pulse sequence used for ^{13}C RGI of solids; b) a ^{13}C 2-dimensional filtered backprojection image of the sample constructed from 18 projections.

is a complicated function of the pulse imperfections, the time between pulses, and the magnitude of each individual inhomogeneous interaction. Independently removing the largest interaction makes the results less sensitive to the pulse sequence parameters.

Figure 2b is a 2-dimensional ^{13}C image of a piece of polycarbonate obtained with the pulse sequence of Fig. 2a. A line drawing of the sample is shown in the inset. The dimensions are 4.5 X 5.5 X 16 mm. The 2-dimensional image was constructed by the filtered backprojection technique [15] from 18 1-dimensional projections taken at 10° intervals. The salient features of the object shown in the inset are evident in the image. Variations in intensity within the image are due to noise and not to real variations in spin density. The spatial resolution as measured from a 1-dimensional projection and based on the resonance linewidth of 75 Hz is 0.15 mm.

Refocused Gradient Imaging of Concentrated Nuclei in Solids

MRI of concentrated spin-1/2 nuclei in solids presents a very different problem than that of dilute nuclei because of homonuclear dipolar broadening. We have previously demonstrated ^{1}H MRI of solids using rf excitation to effect homonuclear dipolar decoupling [7]. Although this generally accounts for the predominant line-broadening mechanism for concentrated nuclei in solids, inhomogeneous broadening can also be a problem. For this reason an imaging technique which simultaneously removes homonuclear dipolar and inhomogeneous broadening is needed.

Removal of the homonuclear dipolar interaction by rf excitation is similar to removal of inhomogeneous interactions described above except that it is not sufficient to simply invert the signs of the spin states. The homonuclear dipole-dipole interaction is described by the second Legendre polynomial, so we generate a series of spin states with three-fold rotation symmetry about the cubic body diagonal to average the interaction to zero [6]. If the series of states ends in the initial state, the pulse sequence can be applied repetitively and the magnetization sampled at the end of each series in a manner similar to that for RGI of dilute nuclei. This is the basic premise of the pulse sequence used in reference [7].

Homonuclear dipolar decoupling pulse sequences also affect the inhomogeneous interactions by making them appear to evolve about a new direction in spin space. This new direction is often referred to as the 'effective' field. For RGI of concentrated nuclei we would like a pulse sequence which provides homonuclear dipolar decoupling as the sequence used in reference [7] and which has an effective field B_{eff} during one half of the sequence and $-B_{eff}$ during the other half [16]. Such a sequence is shown in Fig. 3a. We refer to this type of pulse sequence as a reversed effective field (REF) sequence [17]. All pulses in the sequence are $\pi/2$ pulses. The x, y, $\overline{x}$, and $\overline{y}$ describe the phases of the pulses.

Figure 3b is the 2-dimensional ^{1}H refocused gradient image of the polycarbonate sample imaged in Fig. 2b. As before the image is reconstructed from 18 projections taken at 10° intervals by filtered backprojection. As expected, the image is very similar to the ^{13}C image of Fig. 2b. Small distortions which may be noticeable at the center of the field of view are due to effects of the pulse sequence at zero frequency [17]. The spatial resolution as measured from a 1-dimensional projection and based on a linewidth of 200 Hz is 0.45 mm.

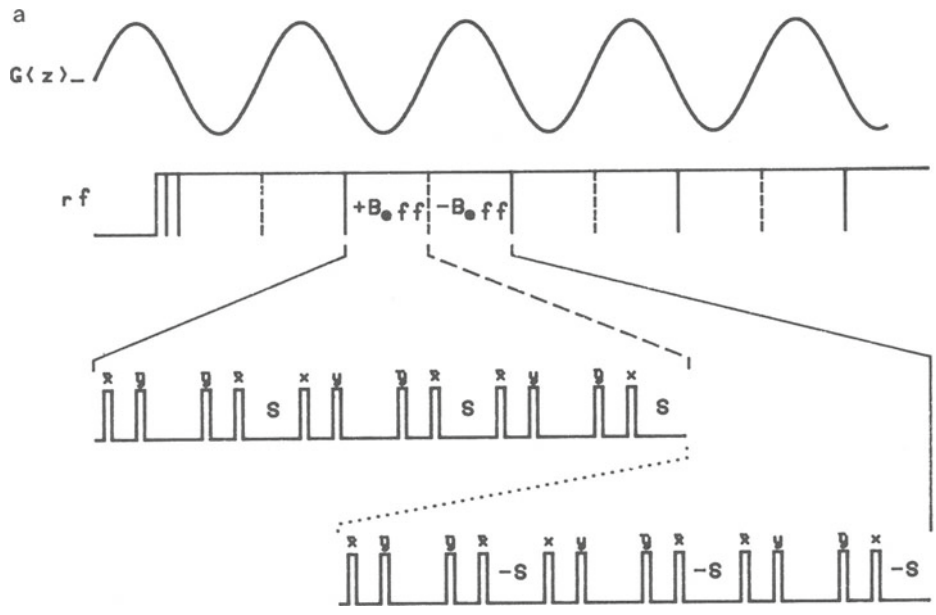

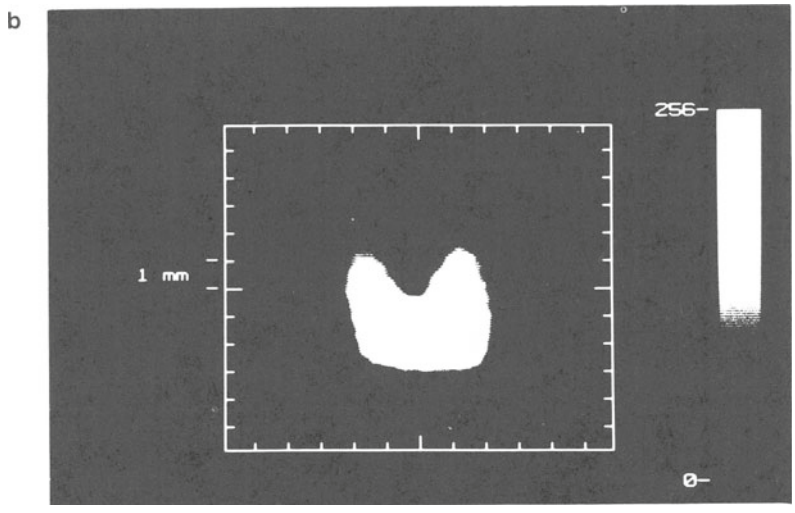

Fig. 3 Refocused gradient imaging of concentrated nuclei in solids. Details of the sample are given in the caption of Fig. 2. a) Pulse sequence for ^{1}H RGI of solids. The x, y, $\overline{x}$, and $\overline{y}$ describe the phases of the rf pulses; b) 2-dimensional ^{1}H filtered backprojection image of the sample of Fig. 2 constructed from 18 projections.

DISCUSSION

As we mentioned earlier, the sensitivity of MRI motivates our use of line narrowing for imaging solids. There are a number of complex factors which determine the actual signal-to-noise ratio of an image. The resonance linewidth is significant in that the sensitivity is linearly dependent on the linewidth and the NMR linewidth can vary by several orders of magnitude from sample to sample. For the examples given above, the ^{1}H linewidth of liquid water was approximately 25 Hz while that of solid polycarbonate was 25 kHz. This represents a three orders of magnitude decrease in sensitivity for the solid sample. The line narrowing used with RGI reduced the polycarbonate linewidth to 200 Hz. With other factors considered and under our experimantal conditions, the sensitivity of RGI is 21 times that of imaging without line narrowing for the ^{1}H image of polycarbonate [17].

In general, imaging of concentrated nuclei is preferred to imaging of dilute nuclei because of the issue of sensitivity. The relative sensitivity of ^{13}C NMR to ^{1}H NMR is normally taken to be approximately 1/5800 [18]. For this reason few reports of MRI of dilute nuclei in solids have appeared [19]. A number of factors increase the sensitivity of RGI of dilute nuclei relative to concentrated nuclei [12]. Taking these factors and the ^{13}C RGI linewidth (75 Hz for polycarbonate) into account, the relative C/H sensitivity is of the order of 1/100 for the polycarbonate image of Fig. 2. While this is still far less sensitive than imaging concentrated nuclei, it demonstrates that imaging dilute nuclei is not only possible but is much more sensitive than expected based only on spectroscopic considerations. This opens up the possibility of MRI of samples which do not contain any concentrated nuclei. Furthermore, since RGI of dilute nuclei is technically much easier to implement than its analogue for concentrated nuclei, it may prove useful in some applications where sensitivity is not an important issue.

We have described techniques for high resolution MRI, of both dilute and concentrated nuclei in solids. These techniques are applicable to most spin-1/2 nuclei including ^{13}C, ^{29}Si, and ^{31}P as dilute nuclei and ^{1}H and ^{19}F as concentrated nuclei. Our preliminary images demonstrate the effectiveness of RGI of solids, although they certainly do not test the ultimate spatial resolution of these techniques.

REFERENCES

1. P. Mansfield and P. C. Morris, "Advances in Magnetic Resonance," Supp. 2, NMR Imaging in Biomedicine, (Academic Press, New York, 1982).
2. W. P. Rothwell, D. R. Holecek, and J. A. Kershaw, J. Polym. Sci.: Polym. Lett. Ed. 22, 241 (1984).
3. J. L. Ackerman, W. A. Ellingson, J. A. Koutcher, and B. R. Rosen, Proceedings, 2nd International Conference on Nondestructive Characterization of Materials, (Montreal, 1986).
4. C. Chang and R. A. Komoroski, Polymer Prep. 29, 94 (1988).
5. J. B. Miller and A. N. Garroway, Review of Progress in Quantitative Nondestructive Evaluation, edited by Donald O. Thompson and Dale E. Chimenti (Plenum Press, New York, 1988), Vol. 7A, pp. 287-294.

6. M. Mehring, "NMR-Basic Principles and Progress," Vol. 11, High Resolution NMR in Solids, 2nd ed., (Springer-Verlag, New York, 1983).
7. G. C. Chingas, J. B. Miller, and A. N. Garroway, J. Magn. Reson. 66, 530 (1986), and references therein.
8. (a) D. G. Cory, J. W. M. van Os, and W. S. Veeman, J. Magn. Reson. 76, 543 (1988); (b) D. G. Cory, A. M. Reichwein, J. W. M. van Os and W. S. Veeman, Chem. Phys. Lett., 143,467 (1988); (c) D. G. Cory and W. S. Veeman, J. Magn. Reson. in press.
9. P. Bendel, IEEE Trans. Med. Imaging MI-4, 114 (1985).
10. J. B. Miller and A. N. Garroway, J. Magn. Reson. 67, 575 (1986).
11. (a) H. Y. Carr and E. M. Purcell, Phys. Rev. 94, 630 (1954); (b) S. Meiboom and D. Gill, Rev. Sci. Instrum. 29, 688 (1958).
12. J. B. Miller and A. N. Garroway, submitted to J. Magn. Reson.
13. A. Pines, M. G. Gibby, and J. S. Waugh, J. Chem. Phys. 59, 569 (1973).
14. L. R. Sarles and R. M. Cotts, Phys. Rev. 111, 853 (1958).
15. R. A. Brooks and G. Di Chiro, Radiology 117, 561 (1975).
16. P. Mansfield and P. K. Grannell, Phys. Rev. B 12, 3618 (1975).
17. J. B. Miller and A. N. Garroway, submitted to J. Magn. Reson.
18. F. W. Wehrli and T. Wirthlin, Interpretation of Carbon-13 NMR Spectra, (Heyden and Son Ltd., London, 1976).
19. N. M. Szeverenyi and G. Maciel, J. Magn. Reson. 60, 460 (1984).